Published in final edited form as:
Mol Cancer Ther. 2014 July ; 13(7): 1729–1739. doi:10.1158/1535-7163.MCT-13-0982.

Anti-*MiR-182* reduces ovarian cancer burden, invasion, and metastasis: An *in vivo* study in orthotopic xenografts of nude mice

Xiaofei Xu[1,2], **Bushra Ayub**[2], **Zhaojian Liu**[2,3], **Vanida Ann Serna**[4,+], **Wenan Qiang**[2,4,5], **Yugang Liu**[2], **Eva Hernando**[6], **Sonya Zabludoff**[7], **Takeshi Kurita**[4,5,+], **Beihua Kong**[1,*], and **Jian-Jun Wei**[2,4,5,*]

[1]Department of Obstetrics and Gynecology, Qilu Hospital, Shandong University, Jinan, Shandong, China

[2]Department of Pathology, Northwestern University School of Medicine, Chicago, IL, USA

[3]Institute of Genetics, Shandong University School of Medicine, Jinan, Shandong, China

[4]Department of Obstetrics and Gynecology, Northwestern University School of Medicine, Chicago, IL, USA

[5]Robert H. Lurie Comprehensive Cancer Center, Northwestern University School of Medicine, Chicago, IL, USA

[6]Department of Pathology, New York University, New York, NY, USA

[7]Regulus Therapeutic, San Diego, USA

Abstract

High-grade serous ovarian carcinoma (HGSOC) is a fatal disease, and its grave outcome is largely due to widespread metastasis at the time of diagnosis. Current chemotherapies reduce tumor burden, but they do not provide long term benefits for cancer patients. The aggressive tumor growth and metastatic behavior characteristic of these tumors demand novel treatment options such as anti-microRNA treatment which is emerging as a potential modality for cancer therapy. *MicroRNA-182 miR-182* overexpression contributes to aggressive ovarian cancer, largely by its negative regulation of multiple tumor suppressor genes involved in tumor growth, invasion, metastasis, and DNA instability. In this study, we examined the therapeutic potential of anti-*miR-182* utilizing the animal orthotopic model to mimic human ovarian cancer using ovarian cancer cells SKOV3 (intrabursal xenografts) and OVCAR3 (IP injection). These models provide a valuable model system for the investigation of ovarian cancer therapy *in vivo*. Through a combination of imaging, histological, and molecular analyses, we found that anti-*miR-182* treatment can significantly reduce tumor burden (size), local invasion, and distant metastasis

[*]Corresponding Authors: Dr. BH Kong, Department of Obstetrics and Gynecology, Qilu Hospital, Shandong University, 107 Wenhuaxi Road, Jinan, Shandong, 250012, China. Tel: +86-531-82169268; kongbeihua@sdu.edu.cn or Dr J-J Wei, Department of Pathology, Northwestern University, School of Medicine, Feinberg 7-334, 251 East Huron Street, Chicago, IL 60611; Telephone: 312-926-1815, Fax: 312-926-3127, jianjun-wei@northwestern.edu.
[+]Current address: Department of Molecular & Cellular Biochemistry, The Comprehensive Cancer Center, Ohio State University Columbus, OH USA

Conflict of Interest Statement: Authors have no conflicts of interest.

compared to its control in both models. The bases of anti-*miR-182* treatment are mainly through the restoration of *miR-182* target expression, including but not limited to BRCA1, FOXO3a, HMGA2 and MTSS1. Overall, our results strongly suggest that anti-*miR-182* can potentially be used as a therapeutic modality in treating HGSOC.

Keywords

Anti-*miR-182*; ovarian cancer; mouse model; metastasis; IVIS

Introduction

Ovarian cancer is the most lethal gynecologic malignancy in women and is the fifth leading cause of cancer-related death. Despite great efforts and progress in surgery and chemotherapy, 5-year survival for advanced-stage ovarian cancer remains only 30%. High-grade serous ovarian carcinoma (HGSOC) is the most aggressive form of ovarian cancer, contributing to the majority of ovarian cancer fatalities due to early invasion and metastasis at the time of diagnosis. The tumor dissemination of HGSOC originates in the contralateral ovary, followed by widespread metastasis within the abdominal cavity, peritoneal organs, and regional lymph nodes (1). Emerging data shows that some of the miRNA dysregulation may contribute to the aggressive metastasis of HGSOC, including *miR-182* (2, 3) and *miR-200* (4, 5) dysregulation. Currently, the targeted miRNA therapy for ovarian cancer invasion and metastasis has yet to be reported.

MiR-182, a member of the *miR-183-96-182* cluster, is overexpressed in HGSOC and associated with tumor growth and invasion in these tumors (2, 6). *MiR-182*-mediated aggressive growth is mostly mediated by the direct regulation of several genes associated with tumor invasion and metastasis (2, 7–9). Moreover, *miR-182* overexpression promotes the invasion and metastasis of several other human cancers (2, 7, 8). Therefore, anti-*miR-182* may provide a beneficial therapy to reduce the tumor burden and metastasis in those malignant neoplasms with *miR-182* overexpression. For example, Hernando's group was the first to provide proof-of-principle of the anti-metastatic potential of anti-*miR-182* in melanoma using a mouse model (10). Compared to other solitary carcinomas, ovarian cancer has its own unique features of tumor growth and metastasis that need to be further studied to develop a specialized therapeutic. Investigation of the therapeutic potential of anti-*miR-182* in a mouse model that mimics the corresponding human ovarian cancer tumors is the initial step to determine the value of miRNA-based gene therapy against human HGSOC.

In this study, we investigate the potential of anti-*miR-182* treatment as an anti-invasion therapeutic strategy for ovarian cancer. We selected two ovarian cancer cell lines overexpressing *miR-182* and prepared mouse xenografts by implanting cancer cells into intrabursally or intraperitoneally. Tumor growth, invasion, and metastasis were evaluated during anti-*miR-182* treatment by luciferase imaging (IVIS system) and histopathology, followed by thorough analysis of *miR-182* expression and target gene expression. We found that anti-*miR-182* treatment could significantly reduce ovarian cancer burden and metastasis

with minimal toxicity. Our study provides a potential therapeutic modality that targets the aggressive tumor growth of HGSOC.

Materials and methods

Ovarian cancer cell line with stable *miR-182* and luciferase transfection

Human ovarian cancer cell lines, SKOV-3 and OVCAR3 were purchased from the ATCC (American Type Culture Collection, Manassas, VA) and stored during early passage. No authentication was done after resuscitation. SKOV3 lines with stable *miR-182* overexpression were prepared off site and are described elsewhere (11). Human FUW-LucNeo (lentivirus) expressing luciferase was prepared in HEK293T cells packaged by pMD2G and psPAX2. Cultured cells (4×10^4) were placed and replaced with 1 mL per well of Opti-MEM I Reduced-Serum Medium containing 12 μg/mL polybrene. 50 μL of concentrated lentiviral particles were added. 48 hours later, fresh medium containing 300 μg/mL G418 was added. Fresh medium containing G418 was replaced every 3 to 4 days. Single colonies were obtained 4 weeks after G418 selection. SKOV3 cells were maintained in McCoy's 5A medium plus 10% fetal bovine serum (FBS, USA Scientific), and OVCAR3 cells with high endogenous miR-182 (12) were cultured in DMEM medium plus 20% FBS and 0.01 mg/mL bovine insulin.

Anti-*miR-182* transient transfection

The anti-*miR-182* and scramble control compounds were provided by Regulus Therapeutics. (San Diego, CA, USA, http://www.regulusrx.com/about-micrornas/). The efficacy of anti-*miR-182 in vitro* was tested in serial dilutions of 20, 40, 60 and 100 nM. In brief, cells were placed in a 6-well plate (2×10^5 per well) in medium without antibiotics. At 70% confluence, cells were transfected with anti-*miR-182*, scrambled control at a concentration of 100 nM, using Lipofectamine 2000 according to the manufacturer's protocol. After transfection, cells were harvested and analyzed at the indicated times.

Matrigel invasion and migration assays

2.5×10^5 SKOV3 cells were seeded into Matrigel-coated upper chambers (BD Biosciences) in McCoy's 5A medium containing 0.5% FBS. The lower chamber of the transwell was filled with culture media containing 10% FBS as a chemo-attractant. After 24 hours, the non-invading cells in the upper chamber were removed with a cotton swab. Cells on the lower surface of the membrane were fixed by 10% formalin, stained by 0.1% crystal violet for 30 minutes, and counted under a light microscope.

For the migration array, OVCAR3 cells (1.5×10^6 cells) transfected with anti-*miR-182* or scramble were seeded into 6-well plate. When cells reached confluence, a scratch was made by a 10-μL tip. The scratches were then recorded at 0 and 48 hour, respectively.

Soft agar colony formation assay

The cells (0.75×10^4 cells) were suspended in 3 ml of culture medium containing 0.3% agar (USB Corporation, OH) and seeded onto a base layer of 3 ml of a 0.6% agar bed in 60-mm tissue culture dishes. The media was changed twice a week. After 3 weeks, colonies were

stained with 0.005% crystal violet and photographed. Colonies >0.1 mm in diameter were counted, and the average numbers (n=3) in each group were calculated.

Cellular proliferation assay

Cells (2×10^3 cells per well) were seeded onto 96-well plates in triplicate. Cell proliferation was monitored by WST (Roche) at different times (0–5 days) according to manufacturer's instructions. Briefly, 10 μL WST were added into each well. After incubation for 4 hours at 37 °C, the absorbance of the samples was measured against a background control using a microplate reader at 450 nm. The cell numbers were calculated as: OD value of different time point/OD_{0h} value × 2000.

Reverse transcription (RT)-polymerase chain reaction (PCR) and real-time PCR

Total RNA was extracted using the mirVanaTM RNA Isolation kit following manufacturer's instructions (Ambion, Austin, TX). 1 μg of total RNA was reverse-transcribed to cDNA using an Advantage RT for PCR Kit (Clontech, Mountain View, CA). MirVana qRT-PCR primers were used to test the expression of miRNA and *U6* was used as a control. For real-time PCR, cDNA was synthesized by SYBR Green real-time PCR master mix (Bio-Rad, Hercules, CA) using a MyiQ and iQ5 real-time PCR Detection System with sequence specific miRNA primers (Supp Table 1).

Western blotting

The rabbit anti-human FOXO3 (EP1949Y) and mouse anti-human BRCA1 antibodies were obtained from EMD Millipore Corporation (Billerica, MA, USA). The mouse anti-human MTSS1 antibody was obtained from Abnova (Walnut, CA, USA). The rabbit anti-human HMGA2 polyclonal antibody was purchased from BioCheck, Inc. (Foster, CA, USA) (Supp. Table 2). Cultured cells were harvested and lysed on ice in a NP40 cell lysis buffer (Invitrogen) supplemented with protease inhibitor cocktail. Total protein (30 μg) was separated by SDS-PAGE and electrotransferred onto polyvinylidene fluoride membrane. The membrane was incubated with primary antibodies overnight at 4°C. The specific horseradish peroxidase-conjugated goat anti-rabbit or goat anti-mouse secondary antibody was used to blot the target proteins, and the secondary antibody was detected by enhanced chemiluminescence ECL detection kit.

Xenografts in nude mice

Female athymic NCr-nu/nu mice (8 weeks old, NCI-Frederick, MD, USA) were used. Mice were maintained in laminar flow rooms, maintaining consistent temperature and humidity and were given free access to water and a normal diet. Experiments were approved by the Institutional Animal Care and Use Committee of Northwestern University.

1) Preparation of cell pellets—SKOV3-*miR-182* cells with luciferase expression were washed twice with PBS. Cell count and viability were performed with the Countess analyzer (Invitrogen) using 0.4% Trypan Blue solution. Cells were suspended into rat type I collagen (6.8 mg/mL, BD Biosciences, San Jose, CA) at 10^6 per 10 μL. The cell-collagen mixture

was then dropped onto a 6-well plate and incubated at 37 °C in a humidified atmosphere of 95% air and 5% CO2. The pellets were incubated overnight as floating cultures.

2) Surgical procedure for implantation of xenografts in intraovarian bursa—8-week-old female athymic NCr-nu/nu nude mice (NCI) were anesthetized by intraperitoneal injection of ketamine/xylazine (90/8 mg/kg) and disinfected with providone iodine prep pads. An incision about 1.0 cm in length was made in the skin just laterally to the midline of the lower back, and the ovary was visible under the muscle layer. After pulling out the left ovary, the ovarian bursa would be identified. A tiny hole was made under microscope, and the cell pellet was grafted into the intrabursa. The pellet was fixed because of the tension of bursa. Ovary was put back in place, and if no bleeding was noted, the incision on the muscle layer and body wall was closed separately.

3) IP injection for OVCAR3—OVCAR3 cells with luciferase expression were suspended in PBS at 1×10^7/mL. The 100 μL cell suspension was then injected intraperitoneally into nude mice using a 25 G needle.

4) Anti-miR-182 treatment—3 days after the ovarian surgery, mice were divided into two groups randomly and administrated intraperitoneally with either anti-*miR-182* (25 mg/kg) or a scramble control with the same chemical modification pattern twice a week (Supp Figure 3A).

5) IVIS monitoring—The tumor growth was monitored using *in vivo* bioluminescence imaging (IVIS, Xenogen Corp./Caliper Life Science Hopkinton, MA, USA) according to the instructions once a week. Briefly, mice were injected intraperitoneally with firefly Luciferin (150 mg/kg, PerkinElmer, Waltham, MA). After 10 minutes, mice were anesthetized by 3% isoflurane, put in the IVIS imaging box, and imaged dorsally. Tumor size was measured by normalized luminescence acquisition (IVIS software).

Necropsy and histologic evaluation

Mice were sacrificed 8 weeks after the implantation of cancer cells. The blood was drawn via the heart 5 minutes after sacrifice, centrifuged at 2000×g at 4°C for 15 minutes to remove the cellular component, and then stored at −80°C for future use. The bilateral ovaries and uterus were then isolated, and tumors in ovaries were measured and photographed. Simultaneously, the other organs were dissected and collected, including spleen, kidneys, liver, intestine, pancreas, omentum, stomach, omentum, pelvic lymph nodes, diaphragm, lungs, and heart. All primary tumor tissue and organs were processed (fixed in 10% formalin, embedded in paraffin) and sectioned for histologic examination. Tumor histology, differentiation, invasion, and metastasis were examined by pathologists. Part of the tumor and liver tissue from each case was frozen at −80°C °C for molecular analysis.

Statistical analysis

All data are presented as means and standard errors of at least 3 independent experiments. Student's t test was used for comparisons between 2 groups of experiments, and one-way

ANOVA analysis was used for comparisons among 3 or more groups. $P < 0.05$ was considered significant.

Results

MiR-182 is overexpressed in the majority of HGSOC (3), and it promotes tumor growth, invasion, and metastasis, mostly mediated by the repression of many tumor suppressors (2, 7). To test whether anti-*miR-182* treatment can be used in ovarian cancer therapy, in this study, we investigated the effects of anti-*miR-182* treatment on tumor growth, invasion, and metastasis of ovarian cancer cells in xenograft experiments using nude mice.

Effects of Anti-*miR-182* treatment on ovarian cancer cells *in vitro*

o evaluate the efficacy of anti-*miR-182* in target gene expression and oncogenic properties in ovarian cancer, we selected three ovarian cancer cell lines (HEY, OVCAR3, and SKOV3) for *in vitro* analysis. Our results showed that OVCAR3 exhibited high endogenous *miR-182* expression (12) whereas HEY and SKOV3 had stable *miR-182* overexpression as the lines were established by lentiviral infection. For all of the tested cell lines, *MiR-182* expression was significantly reduced from 70% to 90% when the cells were treated with 60 μM anti-*miR-182* (Fig. 1A and 1B). Anti-*miR-182* treatment could significantly rescue BRCA1 (breast cancer 1), FOXO3 (forkhead box O3), and MTSS1 (metastasis suppressor 1) expression, thus inhibiting HMGA2 (high mobility group AT-hook 2) expression in SKOV3 and OVCAR3 (no detectable BRCA1 expression) tumor cell lines (Fig. 1A and 1B, $P<0.05$-0.01).

Next, we examined the role of anti-*miR-182* treatment in reducing the *miR-182* mediated oncogenic properties in ovarian cancer cells. In SKOV3 cell lines, administration of anti-*miR-182* significantly reduced tumor cell invasion through Matrigel (Fig. 1C) and anchorage-independent tumor growth (Fig. 1D). These phenotypes could also be observed in ovarian cancer cell lines: HEY (Supp Fig. 1B) and OVCAR3 (Supp Fig. 1C).

Anti-proliferation by anti-*miR-182* has not been previously reported. To further determine whether anti-*miR-182* inhibits cell proliferation, we examined the growth curves of normal and ovarian cancer cell lines and found that anti-*miR-182* constantly inhibited cell proliferation *in vitro* in all of the tested cells (Supp. Fig. 1A). Tumor cell proliferation rate can be further inhibited by combined cisplatin and anti-*miR-182* treatments in both SKOV3-*miR-182* and OVCAR3 tumor cells (Fig. 1E). These findings support that anti-*miR-182* inhibits *miR-182* expression, restores its target genes' expression which reduces *miR-182* mediated tumor growth *in vitro*.

Intrabursal implantation of SKOV3 tumor cells and IP injection of OVCAR3 in nude mice

In the intrabursal *in vivo* study, we chose SKOV3 and OVCAR3 cell lines for the following reasons: 1) SKOV3 is commonly used in xenograft experiments of nude mice for ovarian cancer studies; 2) *miR-182* overexpression in SKOV3 cells promotes metastasis in nude mice (2); 3) OVCAR3 has high endogenous *miR-182* expression (Fig. 1B) a probable HGSOC cell model (13); and 4) anti-*miR-182* can restore its target gene expression and function in both cell lines *in vitro* (Fig. 1A and 1B).

To produce a mouse model that mimics the human ovarian cancer microenvironment, we implanted tumor xenografts in the mouse ovarian intrabursal space. First, we prepared SKOV3 cells with stable *miR-182* and luciferase expression (see Materials and Methods). To implant enough tumor cells (10^6 cells) and to avoid tumor cell leakage in the small space of the intrabursa, we prepared tumor spherical nodules of about 0.2 centimeter in diameter by embedding SKOV3 cells into collagen I matrix (Fig. 2A). The tumor nodules were then implanted into the left ovarian intrabursal space in 8 week old mice (Fig. 2B). The detail for the intrabursal implantation of ovarian cancer is summarized in Fig 2B and Supp Fig. 2A.

As an alternative, the ovarian cancer cell line, OVCAR3 with luciferase overexpression was chosen for IP injection (~10^6 cells per mouse) in nude mice. IP injection has been broadly used in order to mimic human ovarian cancer growth.

The luciferase expression was used as a tracer molecule for *in vivo* imaging analysis (IVIS) of the tumor status. After surgery, the baseline for the tumor cells was examined and documented by IVIS. As shown in Fig. 2C, 2D and Supp Fig. 2B and 2C, all tumor xenografts could be detected on the initial IVIS scanning and were monitored weekly by IVIS.

Anti-*miR-182* treatment reduces Tumor growth *in vivo*

40 mice receiving SKOV3 xenografts were randomly divided into two groups of 20 mice each: control and test. Out of all of the mice, 18 from the control and 19 from the test groups survived at the end of the experiments. A total of 14 mice received IP injection of OVCAR3 tumor cells and were randomly divided (7 mice/group) into control and test groups. All of the mice survived at the experimental end point.

On the third day post-surgery, control mice were treated with scramble and test mice were treated with anti-*miR-182* (dose of 25 mg·kg^{-1} body weight) via intraperitoneal (I.P.) injection twice weekly. Among 19 mice with SKOV3 xenografts from the test group, 4 mice were treated with anti-*miR-182* for one week (short term), and 15 mice were treated for eight weeks (long term) (Supp Fig. 3A). Tumor growth in each mouse (Fig. 3A, Supp Fig. 3B) and average tumor size (Fig. 3B) was monitored by IVIS weekly for up to 8 weeks. No mouse body weight differences were noted between the control and treated groups (Supp Fig. 3C).

The mice with SKOV3 xenografts were euthanized at the end of 8 weeks, and the tumor sizes were further examined and measured in oophorectomy specimens (Fig. 3C and 3D) using the formula $4/3\pi.(d/2^2D/2$, where d is the minor tumor axis and D is the major tumor axis (14). The tumor size and volume in the anti-*miR-182* treatment group (5.42±1.00 mm, 90.59±37.31 mm^3) was significantly smaller than that in the control (8.07±1.74 mm, 310.89±187.12 mm^3) (P<0.001). The treated tumors were reduced by 32.8% (Fig. 3D). The mouse serum level for CA125 was measured by ELISA in the control and test mice. We found that the CA125 level was lower in the test group than that in the control group (P=0.06, Supp Fig. 4B).

The tumor growth rate for OVCAR3 cells in nude mice was detected and scored by IVIS from 0-8 weeks (Fig. 2D and 3F). As shown in Fig. 3E, at the end of the experiment, the tumor size and number of tumors were significantly higher in control group than in mice with anti-*miR-182* treatment ($p<0.01$).

In this study, anti-*miR-182* treatment reduces the tumor growth rate and tumor size. Since several studies (7, 8, 15) showed inconsistent results for *miR-182* mediated tumor growth in breast cancer and melanoma, we want to know whether the reductions in tumor growth and burden by anti-*miR-182* treatment in ovarian cancer cell lines are target specific or a non-specific genotoxic effect. As a result,, we examined several regulators of cell cycle and cell death that are predicted target genes of *miR-182* 16). Real-time PCR analysis revealed that anti-*miR-182* treatment restored several cell cycle genes, including *CDKN1A, CDKN1B, CHEK2, CYLD, FOXO1, PDCD4,* and *RECK* (Fig. 4).

Anti-*miR-182* treatment inhibits metastasis *in vivo*

MiR-182 overexpression promotes tumor metastasis (2, 8, 17). To test whether anti-*miR-182* treatment can prevent metastasis in ovarian cancer, we prepared the xenografts in the mouse ovarian intrabursa to mimic the human ovarian cancer environment, followed by anti-*miR-182* treatment to the mice. Although the IVIS system could be relatively reliable in monitoring tumor growth (Fig. 3), it is not sensitive enough to detect the micro-metastatic tumors in living mice. For example, the incidence of metastatic tumors detected by IVIS at 8 weeks was 28% (5/18) in the control and 7% (1/15) in the test group (Supp Fig. 2C). We found that the metastases detected by IVIS were generally larger than 1 mm in diameter (Fig. 5C). To further evaluate the actual metastatic disease, we collected all of the peritoneal organs, including the liver, spleen, pancreas, gut, lymph nodes, omentum, kidneys, oviducts and uterus as well as the lungs and heart and examined the tissue sections microscopically. In fact, many micro-metastases with the tumor size of 0.2-0.3mm could not be detected by the IVIS system (Fig. 5A and Supp Fig. 5). Overall, 77.8% (14/18) of the control mice and 33.3% (5/15) of the test mice had at least one metastatic lesion. A total of 31 metastases were found in the controls compared to 6 metastases in the treated mice (Supp Table 3). The difference in metastasis between the test and control mice was statistically significant ($P<0.05$, Fig. 5B, Supp. Table 3).

The most common sites of metastatic disease between control and test mice, respectively were the following: kidney (50% (9/18) and 0% (0/15)); spleen (44% (8/18) and 20% (3/15)); omentum (28% (5/18) and 13% (2/15)); pancreas (22% (4/18) and 0% (0/15)); and liver (11% (2/18) and 0% (0/15)) (Fig. 5B). In addition, rare metastases in the diaphragm (1/18) and peritoneal lymph node (1/18) were noted. Notable observations were also the large metastases in the pancreas (Fig. 5C) and metastases in the kidney that was mostly confined to the renal capsule (Fig. 5D). Metastases in the spleen and omentum were summarized in Supp Fig. 5. As opposed to the human, metastasis to the contralateral ovary was rarely seen in the mice and only one metastasis was noted in the control group. No lung metastasis was found, which is similar to human ovarian cancer. Our findings demonstrate that blocking *miR-182* expression can significantly reduce the metastatic disease in ovarian cancer.

Molecular analysis of target gene alterations in xenografts treated by Anti-*miR-182*

To confirm that the reduced tumor burden and metastasis by anti-*miR-182* treatment is target gene specific *in vivo*, we collected the tumor xenografts for molecular analyses. Real-time RT-PCR analysis revealed that *miR-182* expression occurred in very low or non-detectable levels in all tumors treated with anti-*miR-182* in comparison to the control (Fig. 6A). There was more than a 90% reduction of *miR-182* expression. Next, we examined the polycistron cluster of the *miR-182* family, including *miR-96* and *miR-183*. We found that anti-*miR-182* could significantly reduce *miR-183* expression, but not *miR-96* Fig. 6B). Reduction of *miR-182* and *miR-183* was also found in the mouse serum samples (Fig. 6C).

8 tumor xenografts from the control and test groups were randomly selected for *miR-182* target gene expression. Western blot (Fig. 6D and 6E) and qRT-PCR (Supp Fig. 6) analyses revealed that the *miR-182* target genes were restored by anti-*miR-182* treatment. These findings support that a single RNA treatment can correct or restore many dysregulated target genes in tumor cells.

MiR-182 also enhances HMGA2 expression (12). Since LIN28B or MYCN expression are closely associated with HMGA2 overexpression (18), we examined their expression in tumor xenografts with and without anti-*miR-182* treatment, and we found that MYCN expression was significantly reduced in tumors treated by anti-*miR-182* (Supp Fig. 4A) and no change of LIN28B was noted.

Discussion

Mouse models of ovarian cancer have been studied extensively (19), however the majority of the models using ovarian cancer xenografts utilize either subcutaneous (20) or intraperitoneal (21) injection. Recent development of orthotopic mouse models of ovarian cancer intends to inject human ovarian cancer cells directly into the ovarian intrabursa (22) in order to mimic the optimal cancer environment. However, we feel that several technical issues may limit its application, such as the small space of the intrabursa to hold a sufficient cell suspension volume, variability in injected cell numbers among mice or the potential for peritoneal seeding due to leakage. To improve the model, we prepared a solid tumor nodule/pellet rather than a loose cell suspension and then implanted it intrabursally (Figure 2, S Figure 2A). To our knowledge, this is the first attempt to implant tumor cell pellets into the ovarian intrabursa.

Our system has several advantages: preparing the tumor nodule/pellet by embedding tumor cells into the collagen matrix, which allows for a consistent number of tumor cells into the small intrabursa (Figure 2B). During our experiences, no leakage or tumor initiation spread outside of the intrabursa was noted. Furthermore, the ovarian intrabursa functions as a barrier and any tumor cell spread or metastasis requires either invasion through the bursa or the lymphovascular system. To maximize the detection of early and micro-metastatic disease, we examined tumor metastasis and invasion not only by IVIS scan, but also by a thorough histologic examination of all peritoneal organs microscopically (Fig. 5).

MiR-182 overexpression promotes tumor cell invasion and metastasis in various cancer subtypes, including melanoma (7), colon cancer (23), breast cancer (8, 17) and ovarian cancer (2). Further analysis revealed that *miR-182* mediated tumor invasion and metastasis occurred through the regulation of many tumor suppressors and oncogenes, including MTSS1 (2, 8), and MITF (7), HMGA2 (2) and other genes (9, 24–26). MTSS1 and HMGA2 may play a central role in *miR-182* mediated tumor metastasis. MTSS1 inhibits cell motility and invasion of breast cancer cells, which are mediated by the regulation of RhoA to act in cytoskeleton rearrangement and invasion of cancer cells (8). MTSS1 also suppresses stress fiber (F-actin) formation, a critical event of cytoskeleton rearrangement during cancer cell migration and invasion (27). MTSS1 is a specific target gene of *miR-182* (2) and is significantly downregulated in HGSOC(6).

HMGA2 is a well-known oncogene, and its tumorigenic function in ovarian cancer was recently characterized (11). HMGA2 enhances ovarian cancer invasion and metastasis through promoting cell proliferation (28, 29), an epithelial to mesenchymal transition (11, 30). Another *miR-182* target gene, RECK, can be restored by anti-*miR-182* treatment (Fig. 4G). RECK is an inhibitor of the matrix metalloproteinase for invasion (17). A target analysis shows that *miR-182* can bind a large group of functional genes, and its overexpression may impair several normal cellular functions (16). Therefore, blocking *miR-182* expression by anti-*miR-182* treatment will not only rescue some well-known tumor suppressor genes, but also restores the critical biologic functions necessary for cell defenses.

The role of *miR-182* in the regulation of cell proliferation has not been well characterized. In this study, we observed that anti-*miR-182* treatment can consistently reduce tumor cell proliferation *in vitro* (Supp Fig. 1) and tumor growth *in vivo* (Fig. 3). We further confirmed that anti-proliferation by anti-*miR-182* treatment was contributed by restoring several cell cycle negative regulators (16), the *miR-182* target genes in xenograft tumors (Fig. 4). These findings suggest that anti-*miR-182* can reduce tumor burden in ovarian cancer.

MiRNA target therapies have been emerging as a new treatment modality in several human cancers (10, 31). Toxicity of anti-microRNA treatment is a major concern as most microRNAs regulate numerous target genes simultaneously. As part of this study, we are also interested in the toxicity of anti-*miR-182* treatment in host mice. By histologic examination of organs, we did not see significant histological and cytological changes after 8 weeks of treatment in the liver, pancreas, gut, kidneys, spleen, and uterus. But we did note an increase of monocytes in the paraovarian fat pad. Similar findings of an increase in Kupffer cells (modified monocytes) in the liver was also noted (10). The significance of monocytic aggregates remains unclear.

In summary, we investigate the therapeutic potential of anti-*miR-182* in treating ovarian cancer growth, invasion, and metastasis in the mouse model. We were able to evaluate the therapeutic effects at molecular, cellular, and anatomic levels. Our study demonstrates that anti-*miR-182* treatment can significantly reduce the tumor burden of primary tumors and inhibit tumor invasion and metastasis. The efficacy of anti-*miR-182* treatment seems largely mediated by restoring target gene expression. Future studies will focus on examining the

therapeutic potential in treating primary HGSOC from patients' derived xenografts or xenopatients.

Supplementary Material

Refer to Web version on PubMed Central for supplementary material.

Acknowledgments

We are grateful for help from Dr. Eric Marcusson and Regulus Inc, who provided the anti-*miR-182* compounds, constructive information, and technical support for this study. We thank Dr. Wilson Liu for his excellent assistance with the IVIS system and the NU animal facility for mouse care and daily support. We would also acknowledge Stacy Druschitz for editing the manuscript. WQ was partially supported by the Baskes Foundation.

Grant support: NIH NCI (1R21CA167038, JJ Wei) and Dixon translation award (JJ Wei).

Abbreviations list

HGSOC	high-grade serous ovarian carcinoma
BRCA1	breast cancer 1
HMGA2	high mobility group AT-hook 2
MTSS1	metastasis suppressor 1
FOXO3	forkhead box O3
IVIS	in vivo bioluminescence imaging

References

1. Lengyel E. Ovarian cancer development and metastasis. Am J Pathol. 2010; 177:1053–1064. [PubMed: 20651229]
2. Liu Z, Liu J, Segura MF, Shao C, Lee P, Gong Y, et al. MiR-182 overexpression in tumourigenesis of high-grade serous ovarian carcinoma. J Pathol. 2012; 228:204–215. [PubMed: 22322863]
3. McMillen BD, Aponte MM, Liu Z, Helenowski IB, Scholtens DM, Buttin BM, et al. Expression analysis of MIR182 and its associated target genes in advanced ovarian carcinoma. Mod Pathol. 2012
4. Bendoraite A, Knouf EC, Garg KS, Parkin RK, Kroh EM, O'Briant KC, et al. Regulation of miR-200 family microRNAs and ZEB transcription factors in ovarian cancer: evidence supporting a mesothelial-to-epithelial transition. Gynecologic oncology. 2010; 116:117–125. [PubMed: 19854497]
5. Park SM, Gaur AB, Lengyel E, Peter ME. The miR-200 family determines the epithelial phenotype of cancer cells by targeting the E-cadherin repressors ZEB1 and ZEB2. Genes Dev. 2008; 22:894–907. [PubMed: 18381893]
6. McMillen BD, Aponte MM, Liu Z, Helenowski IB, Scholtens DM, Buttin BM, et al. Expression analysis of MIR182 and its associated target genes in advanced ovarian carcinoma. Modern pathology : an official journal of the United States and Canadian Academy of Pathology, Inc. 2012; 25:1644–1653.
7. Segura MF, Hanniford D, Menendez S, Reavie L, Zou X, Alvarez-Diaz S, et al. Aberrant miR-182 expression promotes melanoma metastasis by repressing FOXO3 and microphthalmia-associated transcription factor. Proc Natl Acad Sci U S A. 2009; 106:1814–1819. [PubMed: 19188590]
8. Lei R, Tang J, Zhuang X, Deng R, Li G, Yu J, et al. Suppression of MIM by microRNA-182 activates RhoA and promotes breast cancer metastasis. Oncogene. 2013

9. Hirata H, Ueno K, Shahryari V, Deng G, Tanaka Y, Tabatabai ZL, et al. MicroRNA-182-5p promotes cell invasion and proliferation by down regulating FOXF2, RECK and MTSS1 genes in human prostate cancer. PLoS One. 2013; 8:e55502. [PubMed: 23383207]
10. Huynh C, Segura MF, Gaziel-Sovran A, Menendez S, Darvishian F, Chiriboga L, et al. Efficient in vivo microRNA targeting of liver metastasis. Oncogene. 2011; 30:1481–1488. [PubMed: 21102518]
11. Wu J, Liu Z, Shao C, Gong Y, Hernando E, Lee P, et al. HMGA2 overexpression-induced ovarian surface epithelial transformation is mediated through regulation of EMT genes. Cancer Res. 2011; 71:349–359. [PubMed: 21224353]
12. Liu Z, Liu J, Segura MF, Shao C, Lee P, Gong Y, et al. MiR182 overexpression in tumorigenesis of high-grade ovarian papillary serous carcinoma. J Pathol. 2012
13. Domcke S, Sinha R, Levine DA, Sander C, Schultz N. Evaluating cell lines as tumour models by comparison of genomic profiles. Nature communications. 2013; 4:2126.
14. Galimi F, Torti D, Sassi F, Isella C, Cora D, Gastaldi S, et al. Genetic and expression analysis of MET MACC1, and HGF in metastatic colorectal cancer: response to met inhibition in patient xenografts and pathologic correlations. Clin Cancer Res. 2011; 17:3146–3156. [PubMed: 21447729]
15. Huynh C, Poliseno L, Segura MF, Medicherla R, Haimovic A, Menendez S, et al. The novel gamma secretase inhibitor RO4929097 reduces the tumor initiating potential of melanoma. PLoS One. 2011; 6:e25264. [PubMed: 21980408]
16. Krishnan K, Steptoe AL, Martin HC, Wani S, Nones K, Waddell N, et al. MicroRNA-182-5p targets a network of genes involved in DNA repair. RNA. 2013; 19:230–242. [PubMed: 23249749]
17. Chiang CH, Hou MF, Hung WC. Up-regulation of miR-182 by beta-catenin in breast cancer increases tumorigenicity and invasiveness by targeting the matrix metalloproteinase inhibitor RECK. Biochimica et biophysica acta. 2013; 1830:3067–3076. [PubMed: 23333633]
18. Helland A, Anglesio MS, George J, Cowin PA, Johnstone CN, House CM, et al. Deregulation of MYCN, LIN28B and LET7 in a molecular subtype of aggressive high-grade serous ovarian cancers. PLoS One. 2011; 6:e18064. [PubMed: 21533284]
19. Fong MY, Kakar SS. Ovarian cancer mouse models: a summary of current models and their limitations. Journal of ovarian research. 2009; 2:12. [PubMed: 19781107]
20. Heskamp S, Laverman P, Rosik D, Boschetti F, van der Graaf WT, Oyen WJ, et al. Imaging of human epidermal growth factor receptor type 2 expression with 18F-labeled affibody molecule ZHER2, 2395 in a mouse model for ovarian cancer. Journal of nuclear medicine : official publication, Society of Nuclear Medicine. 2012; 53:146–153.
21. Zacchetti A, Martin F, Luison E, Coliva A, Bombardieri E, Allegretti M, et al. Antitumor effects of a human dimeric antibody fragment 131I-AFRA-DFM5.3 in a mouse model for ovarian cancer. Journal of nuclear medicine : official publication, Society of Nuclear Medicine. 2011; 52:1938–1946.
22. Cordero AB, Kwon Y, Hua X, Godwin AK. In vivo imaging and therapeutic treatments in an orthotopic mouse model of ovarian cancer. Journal of visualized experiments : JoVE. 2010
23. Liu H, Du L, Wen Z, Yang Y, Li J, Wang L, et al. Up-regulation of miR-182 expression in colorectal cancer tissues and its prognostic value. International journal of colorectal disease. 2013; 28:697–703. [PubMed: 23474644]
24. Gu C, Li X, Tan Q, Wang Z, Chen L, Liu Y. MiR-183 family regulates chloride intracellular channel 5 expression in inner ear hair cells. Toxicol In Vitro. 2013; 27:486–491. [PubMed: 22889583]
25. Hirata H, Ueno K, Shahryari V, Tanaka Y, Tabatabai ZL, Hinoda Y, et al. Oncogenic miRNA-182-5p targets Smad4 and RECK in human bladder cancer. PLoS One. 2012; 7:e51056. [PubMed: 23226455]
26. Song L, Liu L, Wu Z, Li Y, Ying Z, Lin C, et al. TGF-beta induces miR-182 to sustain NF-kappaB activation in glioma subsets. The Journal of clinical investigation. 2012; 122:3563–3578. [PubMed: 23006329]

27. Saarikangas J, Mattila PK, Varjosalo M, Bovellan M, Hakanen J, Calzada-Wack J, et al. Missing-in-metastasis MIM/MTSS1 promotes actin assembly at intercellular junctions and is required for integrity of kidney epithelia. J Cell Sci. 2011; 124:1245–1255. [PubMed: 21406566]

28. Integrated genomic analyses of ovarian carcinoma. Nature. 2011; 474:609–615. [PubMed: 21720365]

29. Fedele M, Pierantoni GM, Visone R, Fusco A. Critical role of the HMGA2 gene in pituitary adenomas. Cell Cycle. 2006; 5:2045–2048. [PubMed: 16969098]

30. Wu J, Wei JJ. HMGA2 and high-grade serous ovarian carcinoma. J Mol Med (Berl). 2013; 91:1155–1165. [PubMed: 23686260]

31. Ma L, Reinhardt F, Pan E, Soutschek J, Bhat B, Marcusson EG, et al. Therapeutic silencing of miR-10b inhibits metastasis in a mouse mammary tumor model. Nature biotechnology. 2010; 28:341–347.

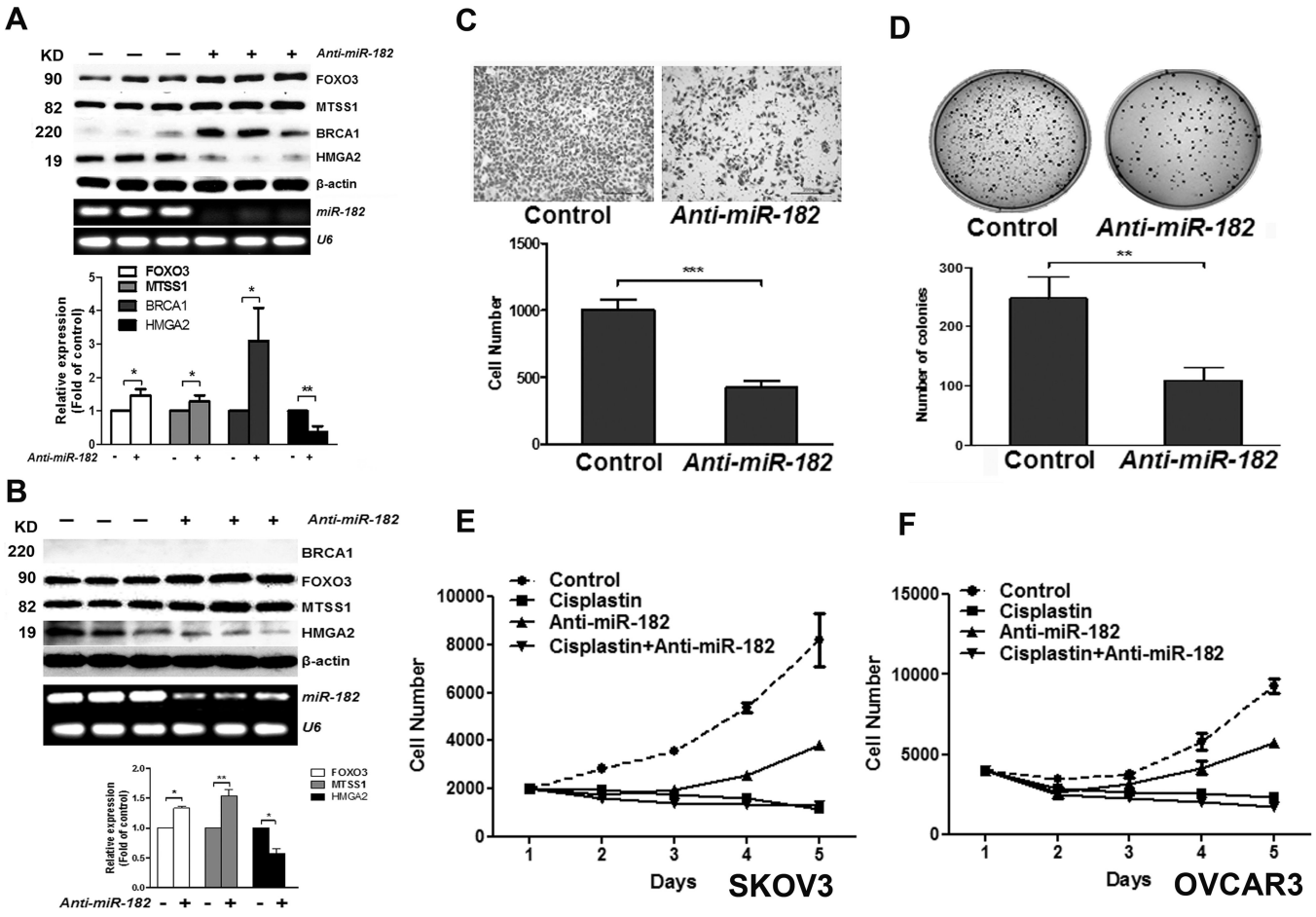

Figure 1.

Anti-*miR-182* treatment rescues the *miR-182* target gene expression and restores tumor cell growth and invasion in ovarian cancer cell line *in vitro*. ***A-B***. Expression of *miR-182* and four target genes in SKOV3 (*A*) and OVCAR3 (*B*) with anti-*miR-182* treatment was presented by Western blot and RT-PCR. β-actin and *U6* was used as protein and RNA loading controls. The average levels of proteins (open box: FOXO3, light gray: MTSS1, dark gray: BRCA1 and black box: HMGA2) were shown below the blotting. ***C*** and ***D***. SKOV3 cell invasion by Mitragel (***C***) and anchorage-independent tumor cell growth by soft agar (***D***) were significantly different between Anti-*miR-182* and control. ***E*** and ***F***. Growth curve showed the treatment effects in SKOV3 (***E***) and OVCAR3 (***F***) cell proliferation in control, cisplatin, anti-*miR-182* and combined cisplatin and anti-*miR-182*. *: $P<0.05$, **: $P<0.01$, ***:$P< 0.001$.

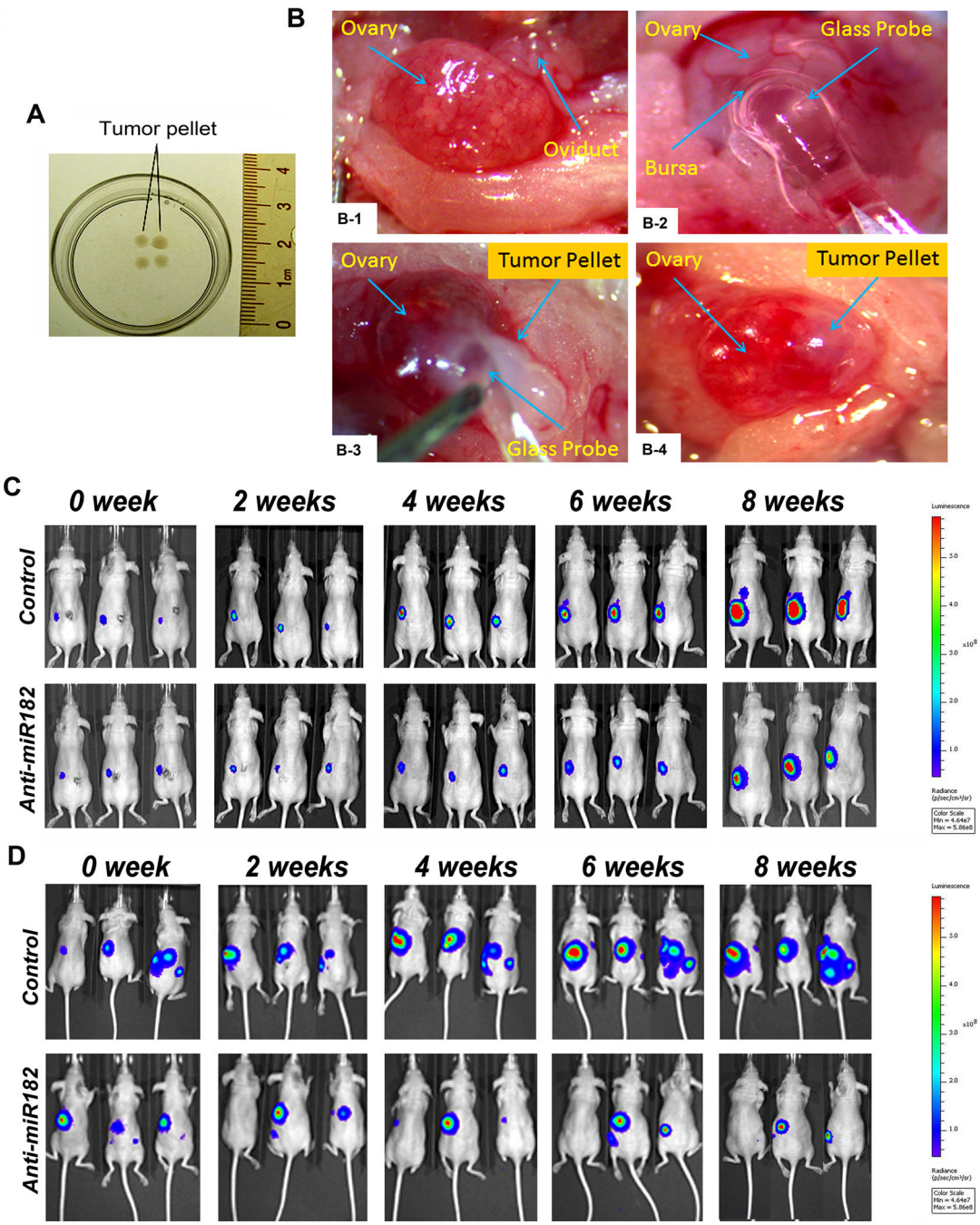

Figure 2.

Orthotopic mouse model of ovarian cancer. ***A***. A photograph illustrated SKOV3 tumor cell pellets embedded in Collagen IV matrix and ready for implantation. ***B***. Photographs illustrated the key steps inserting SKOV3 tumor cell pellet into the ovarian intrabursal space (for detail, please refer to Materials and Methods). After the ovary is exposed (*B-1*), a small hole was cut in the bursa for glass probe insertion (*B-2*), followed by inserting a tumor pellet into the ovarian intrabursa space with the aid of a glass probe (*B-3*), and finally, an intact tumor pellet was completely implanted into ovarian bursa (*B-4*). ***C*** and ***D***. Photographs

illustrate three examples of tumor images by IVIS for intrabursal (SKOV3) and IP injection (OVCAR3) xenografts in different time points between day 0 and 8 weeks (from left to right). Color bars represented tumor cell intensity from low (blue) to high (red). Tumor xenografts were visible in both control (upper panel) and test (lower panel) mice at 0 week.

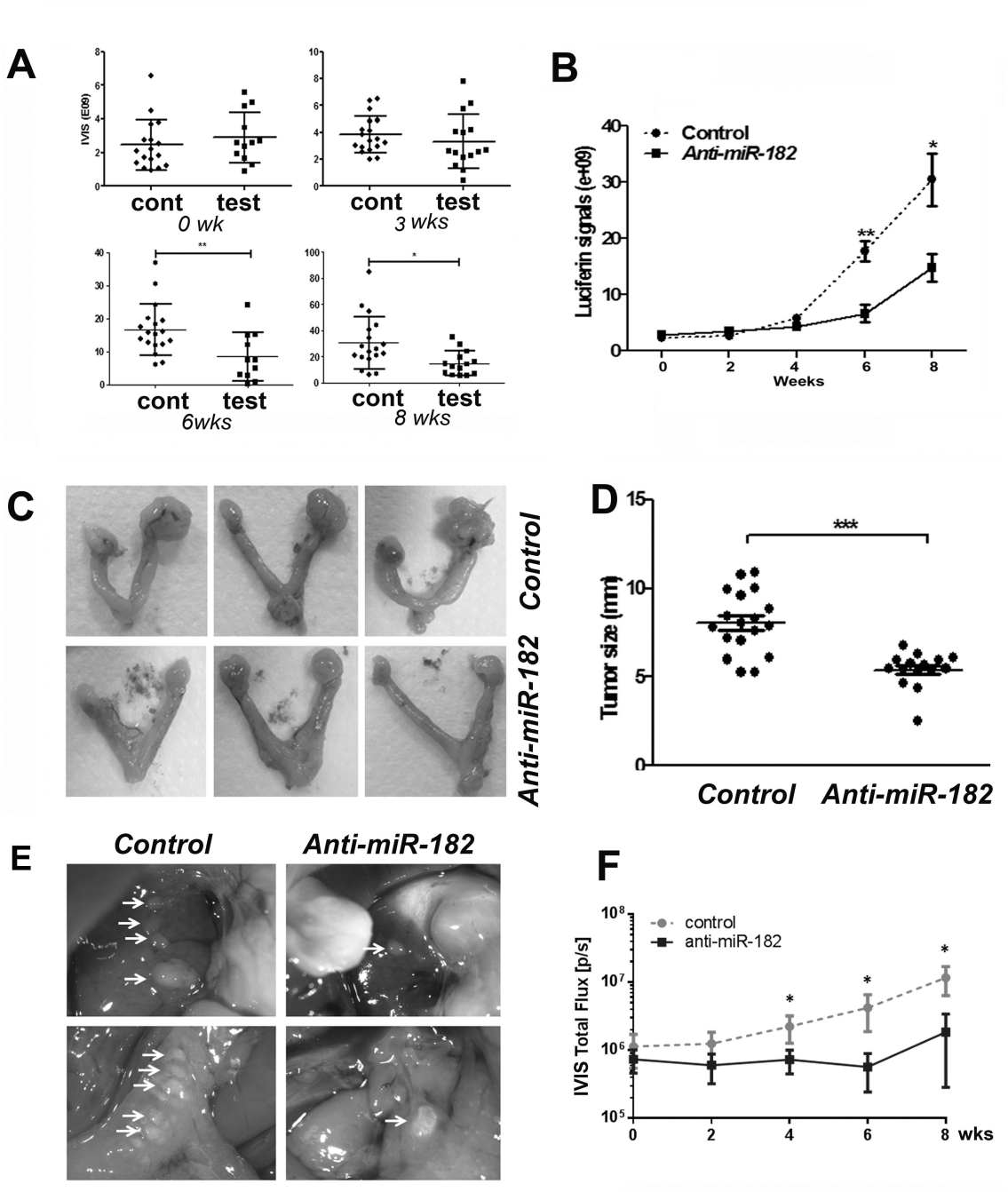

Figure 3.

Quantitative analyses of ovarian cancer growths in xenografts of nude mice. ***A*** and ***B***. Dotplot analysis (***A***) and growth curve (***B***) represented SKOV3 tumor growth rate in each individual xenograft and in each group detected by IVIS scan at 0 to 8 weeks. A total of 18 controls (round dots) and 15 tested (square dots) were used. ***C***. Photographs illustrated some examples of gross appearance of ovarian tumor xenografts in test (bottom) and control (top) mice at the end of 8 weeks. ***D***. The dot plots illustrated the actual tumor sizes (by the largest dimension in millimeter, y-axis) in control and test mice. ***E***. Photographs illustrated

xenograft OVCAR3 tumor nodules on liver (upper) and gut (bottom) in mice of control and anti-*miR-182* treatment at 8 weeks. ***F***. The growth curve represented the tumor growth rate of OVCAR3 cell xenografts in control (n=7) and test (n=7) mice measured by IVIS at weeks of 0 to 8 weeks. *: $P<0.05$, **: $P<0.01$, ***:$P< 0.001$.

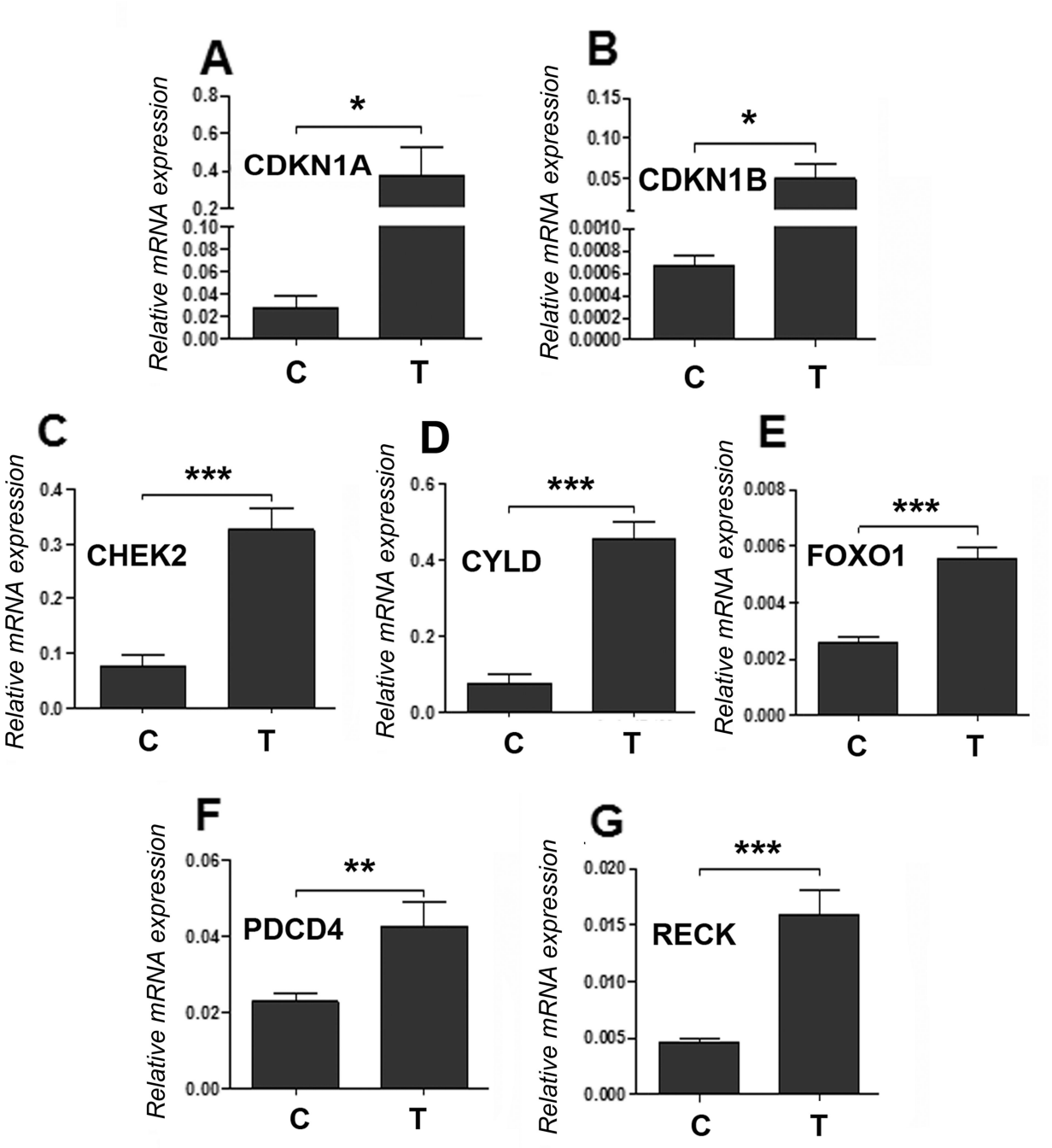

Figure 4.

Anti-*miR-182* restores several antiproliferation gene expressions in tumor cells *in vivo*. ***A-G***. Expression of seven *miR-182* predicted target genes (labeled on left upper corner) were examined by real-time RT-PCR in randomly selected xenograft tumors from control (C) and test (T) mice (n=4 from each). β-actin was used to normalize the expression values. *: $P<0.05$, **: $P<0.01$, ***:$P< 0.001$.

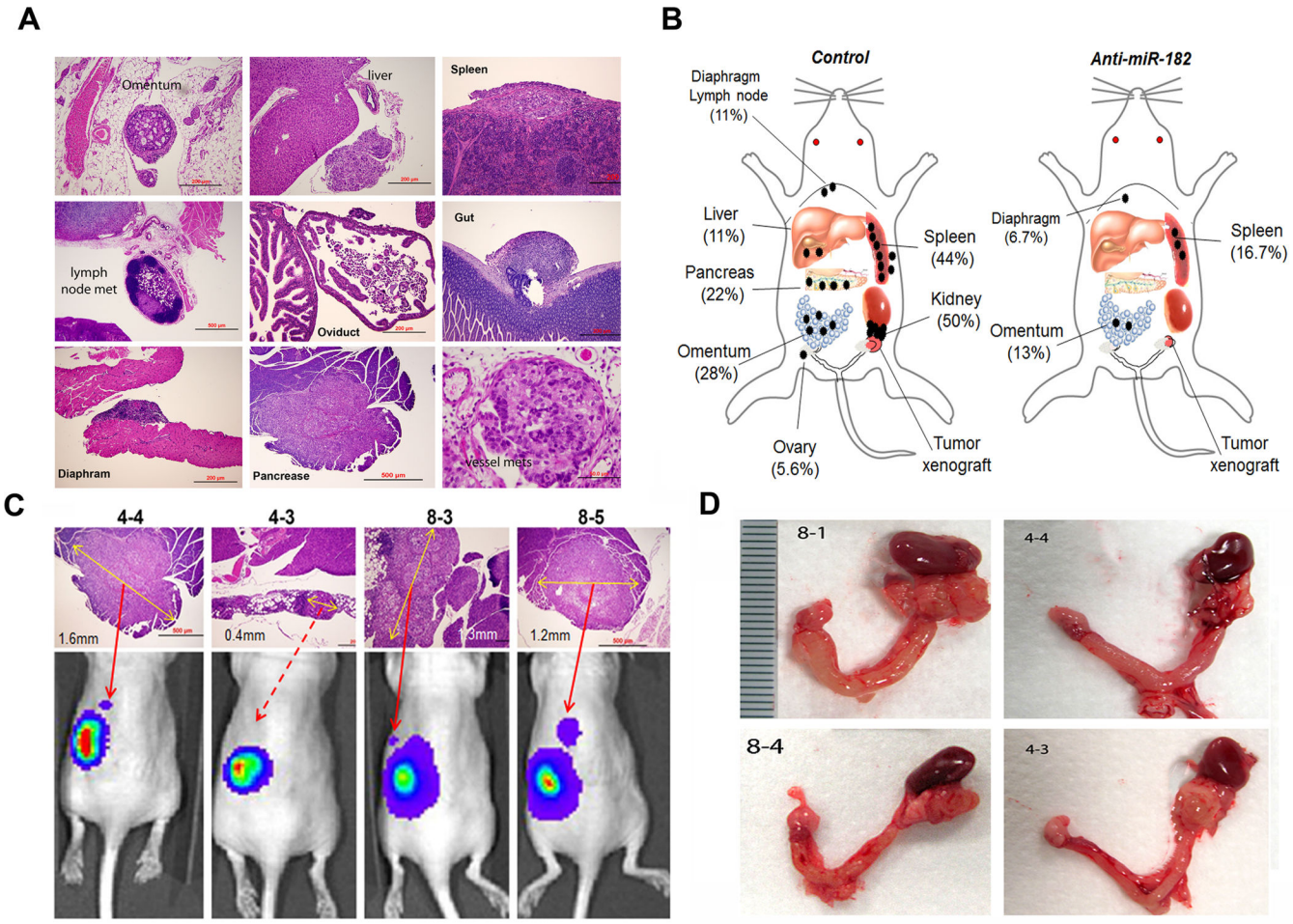

Figure 5.

The distribution and frequency of the metastatic disease in orthotopic mice of SKOV3 cells. The metastatic tumor nodules were examined and identified by histologic examination of all peritoneal organs in control and test groups of mice. ***A***. Photomicrographs illustrated examples of the metastatic carcinomas in different anatomic sites of peritoneal organs, including the omentum, liver, spleen, pancreas, gut, diaphragm, and lymph node. ***B.*** The depicted sketch diagram illustrated the sites (indicated by labels and bar) and frequencies (in percentage) of metastatic disease in peritoneal organs in control and anti-*miR-182* treated mice. ***C***. Histology and IVIS spectrum comparison of four pancreatic metastases that were exclusively identified in control group. The actual tumor size was labeled with a yellow arrow line ***D***. Photographs illustrated some examples of ovarian cancer extending and adhering to ipsilateral kidney that were exclusively seen in control mice.

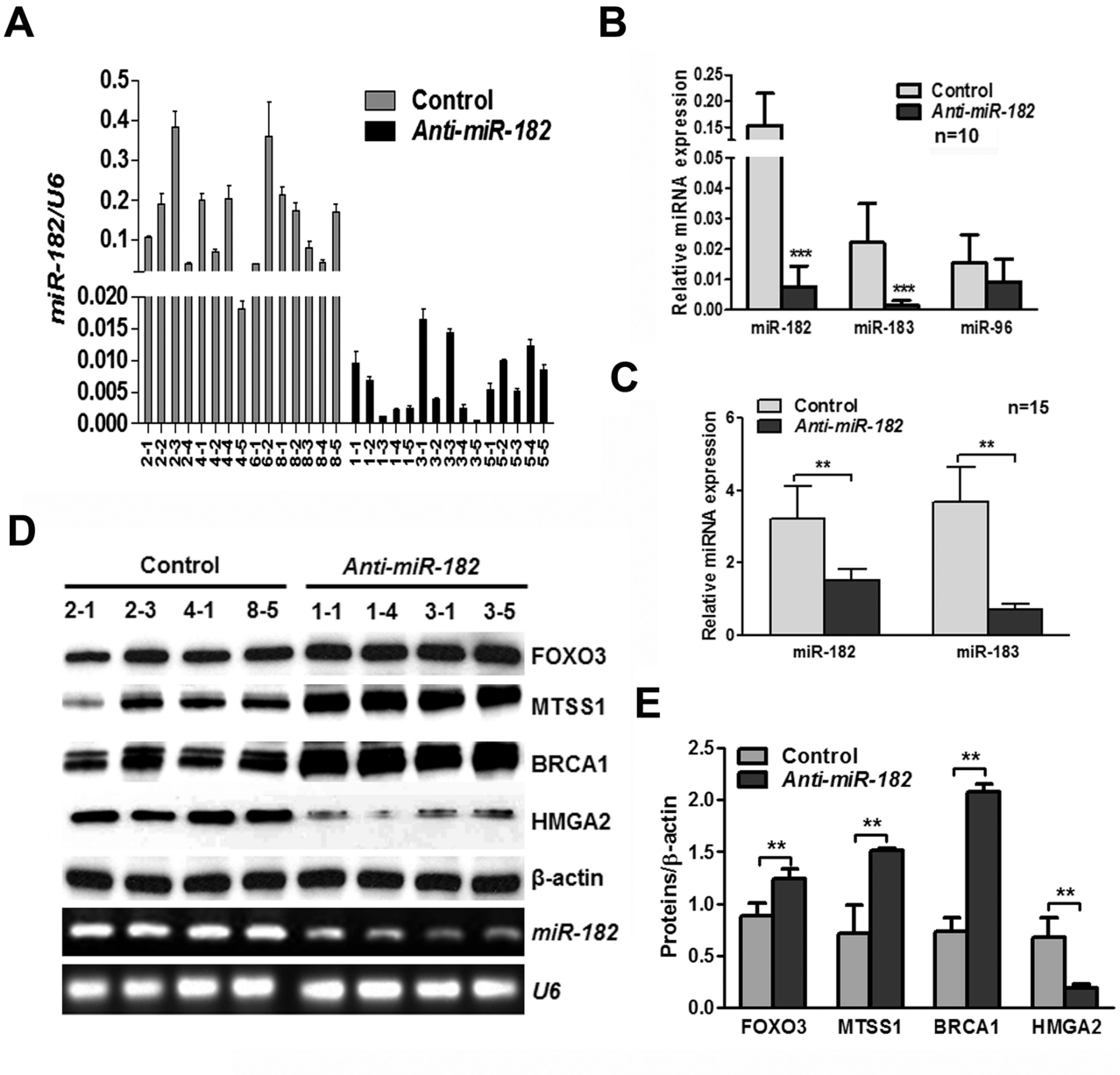

Figure 6.

Gene expression analysis of *miR-182* and its target genes in SKOV3 xenografts with and without *miR-182* treatment. ***A***. Mature *miR-182* expression in tumor xenografts from control (light gray bars, n=15) and anti-miR-182 treated (dark black bars, n=15) mice. ***B***. Histobars displayed the relative expression levels of mature *miR-182* and its polycistron gene cluster of *miR-183* and *miR-96* in tumors of control and test tumors (n=10). C. The levels of mouse mature *miR-182* and *miR-183* expression were detected by real-time RT-PCR in mouse serum. ***D***. and ***E***. Western blot ***D*** and quantitative ***E*** analysis of four *miR-182* major target gene (indicated by labels) expression were illustrated in tumors of control and test (anti-*miR-182*) mice. *: $P<0.05$, **: $P<0.01$, ***:$P< 0.001$.